第 31 卷 第 1 期 高 能 物 理 与 核 物 理 Vol. 31, No. 1
2007 年 1 月 HIGH ENERGY PHYSICS AND NUCLEAR PHYSICS Jan., 2007

Systematic Behavior of Isospin Effect in Fragmentation Reactions*

FANG De-Qing[1)] MA Yu-Gang MA Chun-Wang ZHONG Chen CAI Xiang-Zhou CHEN Jin-Gen GUO Wei SU Qian-Min TIAN Wen-Dong WANG Kun YAN Ting-Zhi SHEN Wen-Qing

(Shanghai Institute of Applied Physics, CAS, Shanghai 201800, China)

Abstract The isospin effect and isoscaling behaviors in projectile fragmentation reactions have been systematically investigated by a modified statistical abrasion-ablation (SAA) model. The normalized peak difference and reduced isoscaling parameters are found to decrease with $(Z_{\rm proj}-Z)/Z_{\rm proj}$ or $(N_{\rm proj}-N)/N_{\rm proj}$ exponentially and have no dependence on the size of reaction systems. It is pointed out that the reduced isoscaling parameters can be used as an observable to study excitation extent of system and asymmetric nuclear equation of state in heavy ion collisions.

Key words statistical abrasion-ablation model, fragmentation reaction, isospin effect

1 Introduction

The process of projectile fragmentation has been studied extensively for investigation of reaction mechanisms in heavy ion collisions at intermediate and high energies[1—7]. It is also one of the most important methods to produce exotic nuclei. Recent advances in experiments using radioactive ion beams with large neutron or proton excess have lead to the discovery of the halo structure[8, 9]. Since then interest in the study of very neutron-rich and proton-rich nuclei has grown due to their anomalous structures. In addition, the study of isospin physics has become a very popular topic in nuclear physics. The isospin effects of various physical phenomena, such as multifragmentation, flow, pre-equilibrium nucleon emission, etc., have been extensively reported[10—17]. The studies have shown that isospin effect exists in nuclear reactions induced by exotic nuclei but it may disappear under certain conditions. Our previous calculations by using the modified statistical abrasion-ablation (SAA) model have demonstrated that the fragment isotopic distribution shifts toward the neutron-rich side for neutron-rich projectile, but the shift decreases with the increase of the parameter $(Z_{\rm proj}-Z)/Z_{\rm proj}$ or the violence of the nuclear reaction. This isospin effect of fragmentation reaction on the fragment isotopic distribution will disappear when $(Z_{\rm proj}-Z)/Z_{\rm proj}$ becomes larger than 0.5[18, 19].

Recently, isoscaling behavior for light fragments produced in the multifragmentation of very hot source has been extensively investigated[20—23]. The scaling law relates ratios of isotope yields measured in two different nuclear reactions, 1 and 2, $R_{21}(N,Z)=Y_2(N,Z)/Y_1(N,Z)$. In multifragmentation events, such ratios are shown to obey an exponential dependence on the neutron number N or proton number Z of the isotopes or isotones characterized by three parameters α, β and C[20]:

$$R_{21}(N,Z)=\frac{Y_2(N,Z)}{Y_1(N,Z)}=C\exp(\alpha N+\beta Z). \quad (1)$$

Here C is an overall normalization constant. In the

Received 21 April 2006, Revised 27 June 2006

* Supported by National Natural Science Foundation of China (10405032, 10535010, 10405033, 10475108, 10328259, 10135030), Shanghai Development Foundation for Science and Technology (06QA14062, 05XD14021, 03QA14066), and Major State Basic Research Development Program (G200077404)

1) E-mail: dqfang@sinap.ac.cn

grand-canonical limit, α and β will have the form,

$$\alpha=\frac{4C_{\rm sym}}{T}\Delta\left[\left(\frac{Z}{A}\right)^2\right]=\frac{4C_{\rm sym}}{T}\left[\left(\frac{Z}{A}\right)_1^2-\left(\frac{Z}{A}\right)_2^2\right] \quad (2)$$

and

$$\beta=\frac{4C_{\rm sym}}{T}\Delta\left[\left(\frac{N}{A}\right)^2\right]=\frac{4C_{\rm sym}}{T}\left[\left(\frac{N}{A}\right)_1^2-\left(\frac{N}{A}\right)_2^2\right], \quad (3)$$

where $C_{\rm sym}$ is symmetry energy coefficient (MeV), $\left(\frac{Z}{A}\right)_i^2$ or $\left(\frac{N}{A}\right)_i^2$ (i=1,2) means the square of Z or N over A for system 1 and 2. T is the temperature of the system in MeV. This behavior is attributed to the difference of isospin asymmetry between two reaction systems in similar nuclear temperature. It can be used to probe the isospin dependent nuclear equation of state by the studies of isoscaling[20—29]. So far, the isoscaling behavior has been studied experimentally and theoretically for different reaction mechanisms. However, most studies focus on the isoscaling behaviors for light particles with Z=2—8. A few studies on the heavy projectile-like residues in deep elastic collisions and fission fragments have been reported[30—34]. In this paper, we will present our studies on systematic behaviors of the isospin effect as well as isoscaling features for projectile-like fragments in the framework of statistical abrasion-ablation model[7].

2 Model description

The statistical abrasion-ablation model can describe the isotopic distribution well[7]. In the SAA model, the nuclear reaction is described in two stages which occur in two distinctly different time scales. The first abrasion stage is fragmentation reaction which describes the production of the pre-fragment with certain amount of excitation energy through the independent nucleon-nucleon collisions in the overlap zone of the colliding nuclei. The collisions are described by a picture of interacting tubes. Assuming a binomial distribution for the absorbed projectile neutrons and protons in the interaction of a specific pair of tubes, the distributions of the total abraded neutrons and protons are determined. For an infinitesimal tube in the projectile, the transmission probabilities for neutrons (protons) at a given impact parameter b are calculated by[7]

$$t_{\rm k}(r-b)=\exp\left\{-[D_{\rm n}^{\rm T}(r-b)\sigma_{\rm nk}+D_{\rm p}^{\rm T}(r-b)\sigma_{\rm pk}]\right\}\ , \quad (4)$$

where $D^{\rm T}$ is the thickness function of the target, which is normalized by $\int {\rm d}^2rD_{\rm n}^{\rm T}=N^{\rm T}$ and $\int {\rm d}^2rD_{\rm p}^{\rm T}=Z^{\rm T}$ with $N^{\rm T}$ and $Z^{\rm T}$ referring to the neutron and proton number in the target respectively, the vectors r and b are defined in the plane perpendicular to beam, and $\sigma_{\rm k'k}$ is the free nucleon-nucleon cross sections (k$'$, k=n for neutron and k$'$, k=p for proton). The thickness function of the target is given by

$$D_{\rm k}^{\rm T}(r)=\int_{-\infty}^{+\infty}{\rm d}z\rho_{\rm k}((r^2+z^2)^{1/2})\ , \quad (5)$$

with $\rho_{\rm k}$ being the neutron (proton) density distribution of the target. So the average abraded mass at a given impact parameter b is calculated by the expression

$$\langle\Delta A(b)\rangle = \int{\rm d}^2rD_{\rm n}^{\rm P}(r)[1-t_{\rm n}(r-b)]+\int{\rm d}^2rD_{\rm p}^{\rm P}(r)[1-t_{\rm p}(r-b)]\ . \quad (6)$$

The excitation energy of projectile spectator is estimated by a simple relation of $E^*=13.3\langle\Delta A(b)\rangle$MeV where 13.3 is a mean excitation energy due to an abraded nucleon from the initial projectile estimated by the particle-hole pair model[35]. In the second evaporation stage the system reorganizes due to excitation, which means it deexcites and thermalizes by the cascade evaporation of light particles. By introducing in-medium nucleon-nucleon cross section and optimizing computational method proposed by our group given in Ref. [18,19,36,37], it can give a good agreement with the experimental isotopic distributions[18, 19, 37]. The isospin effect and its disappearance in projectile fragmentation for ^{36,40}Ar at intermediate energies have been predicted by this model and confirmed by experimental data[19]. In the SAA model, there is no direct information of the nuclear and symmetry potential. But the approximation and treatment of the nuclear collision in the model include the effect of the potential. In this model, different density is used for neutron and proton. The collision processes of neutron and proton are treated separately and locally. Thus it will give a more realistic mass and charge distribution for the produced fragments and better description for the isospin effect and isoscaling phenomena. Since the symmetry energy is related to the isoscaling parameters according to Eqs. (2) and (3), so it is still possible to obtain some reasonable conclusions through the combination of experimental data and calculations by the SAA model.

3 Calculation and discussion

In order to do a systematic study of the isospin effect in projectile fragmentation, reactions of $^{40/36}$Ar, $^{48/40}$Ca, $^{64/58}$Ni, $^{86/78}$Kr, $^{124/112}$Sn and $^{129/136}$Xe on ^{112}Sn at 60AMeV are simulated by the SAA model. The isotope distributions for selected charge numbers after evaporation from $^{124/112}$Sn+^{112}Sn are shown in Fig. 1. The model predicts that the fragment isotopic distribution for a fixed charge number Z shifts towards neutron-rich side for the neutron-rich projectile. The shift becomes small with the increase of the charge difference between the produced isotope and projectile. We extract the peak position by Gaussian fits to the fragment isotopic distribution for each charge number Z. The normalized difference of the peak position from two projectiles $\Delta A_{\rm peak}/\Delta A_{\rm proj}$ as a function of $(Z_{\rm proj}-Z)/Z_{\rm proj}$ are shown in Fig. 2. Here $\Delta A_{\rm proj}$ is the mass number difference between the two projectiles with the same Z and $\Delta A_{\rm peak}$ is the peak position difference of the fragment isotopic distribution produced by these two projectiles. The parameter $(Z_{\rm proj}-Z)/Z_{\rm proj}$ can reflect the violence of the collision[19]. For cold fragments after evaporation, $\Delta A_{\rm peak}/\Delta A_{\rm proj}$ exponentially decreases as the increase of $(Z_{\rm proj}-Z)/Z_{\rm proj}$ which is the same as our previous conclusions. The dependence of $\Delta A_{\rm peak}/\Delta A_{\rm proj}$ on $(Z_{\rm proj}-Z)/Z_{\rm proj}$ shows a slight difference among different size projectiles when $(Z_{\rm proj}-Z)/Z_{\rm proj}$ is small. For comparison, the same plot but for hot fragments before evaporation is shown in the inset. In this case, $\Delta A_{\rm peak}/\Delta A_{\rm proj}$ decreases linearly with $(Z_{\rm proj}-Z)/Z_{\rm proj}$ which is mostly resulted from the geometrical effect and their values among different size projectiles show no significant difference. It looks that the evaporation effect plays an important role for the final projectile-like fragment and breaks the $\Delta A_{\rm proj}$ scaling at lower $(Z_{\rm proj}-Z)/Z_{\rm proj}$ slightly.

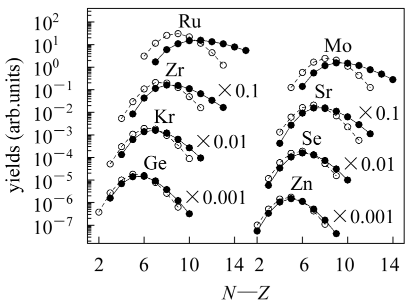

Fig. 1. The isotope distributions of selected charge numbers for cold fragments from $^{124/112}$Sn+^{112}Sn. The open circles are for ^{112}Sn and the solid circles are for ^{124}Sn. The lines serve to guide the eye.

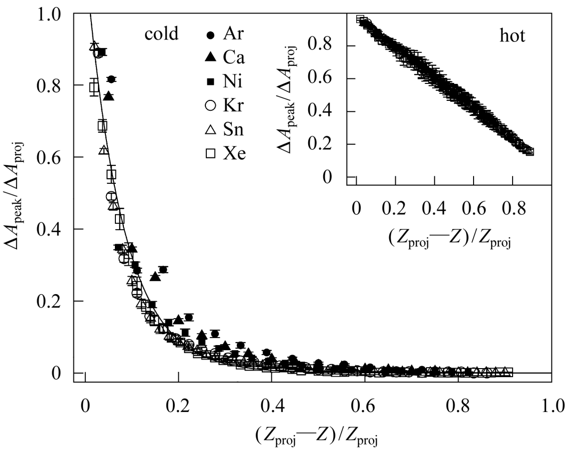

Fig. 2. The normalized peak difference $\Delta A_{\rm peak}/\Delta A_{\rm proj}$ of the fragment isotopic distribution as a function of $(Z_{\rm proj}-Z)/Z_{\rm proj}$ after evaporation. Different symbols are used for projectiles with different Z. The solid lines are the fitted results by an exponential decay function. The inset is the plot for hot fragments before evaporation.

To study systematic behaviors of the isoscaling phenomena, the yield ratios $R_{21}(N,Z)$ are made using the convention that index 2 refers to the more neutron-rich system and index 1 to the less neutron-rich one. As an example, Fig. 3 shows the yield ratios $R_{21}(N,Z)$ of cold projectile-like fragments as a function of neutron number N for selected isotopes from

$^{124/112}$Sn+^{112}Sn reactions in log-scale. From Fig. 3, we observe that the ratio for each isotope Z (from 38 to 49) exhibits a remarkable exponential behavior. For each isotope (Z), an exponential function form $C\exp(\alpha N)$ is used to fit the calculated points and the parameters α are obtained for each isotopes. Analogous behavior is observed for each isotone (N), an exponential function form $C'\exp(\beta Z)$ is used to fit the calculated points and the parameters β are obtained for each isotones.

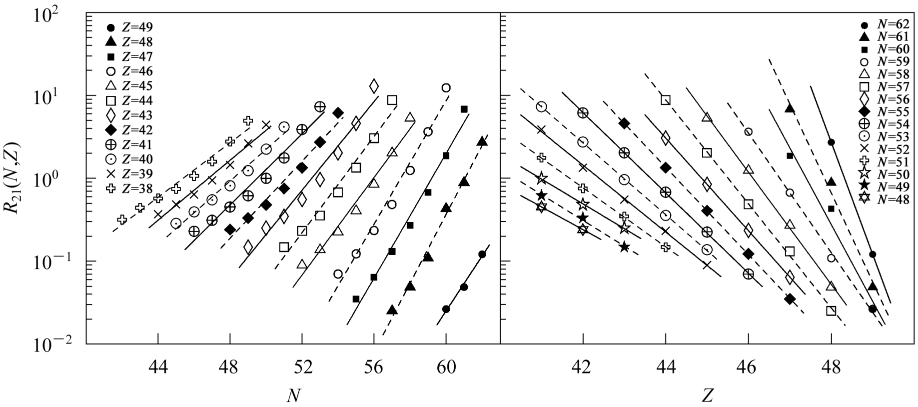

Fig. 3. Yield ratios $R_{21}(N,Z)$ of fragments from the reactions of $^{124/112}$Sn+^{112}Sn at 60AMeV versus N for the selected isotopes (left panel) and Z for the selected isotones (right panel). Different symbols are used for different isotopes and isotones as shown in the legend. The lines represent the exponential fits. For details see text.

In Fig. 4, we present the extracted slope parameters α (upper panel) and $|\beta|$ (lower panel) of the exponential fits as a function of $(Z_{\rm proj}-Z)/Z_{\rm proj}$ or $(N_{\rm proj}-N)/N_{\rm proj}$ for the cold fragments. Here $N_{\rm proj}$ refers to the neutron number of the less neutron-rich projectile. In Fig. 4, α and $|\beta|$ show a decreasing trend with the increasing of $(Z_{\rm proj}-Z)/Z_{\rm proj}$ or $(N_{\rm proj}-N)/N_{\rm proj}$. But the values of α and $|\beta|$ are quite different from different reaction systems. For hot fragments shown in the insets, a slower decrease trend is also observed. The excitation energy and evaporation effect are the main reason for the decrease of the isoscaling parameters in our calculations. For cold fragments, the dependence of the isoscaling parameters on Z is different with the data in Ref. [30], but is similar with the results in Ref. [38]. In the experimental data at 600A MeV in Ref. [38], projectile fragmentation is the main reaction mechanism. While the results around 25A MeV in Ref. [30] are mainly from deep inelastic collisions. Our calculations are performed at 60A MeV, but we have found that there is almost no incident energy dependence for the isoscaling parameters in projectile fragmentation. So our calculated results are similar to the projectile fragmentation data at high energy.

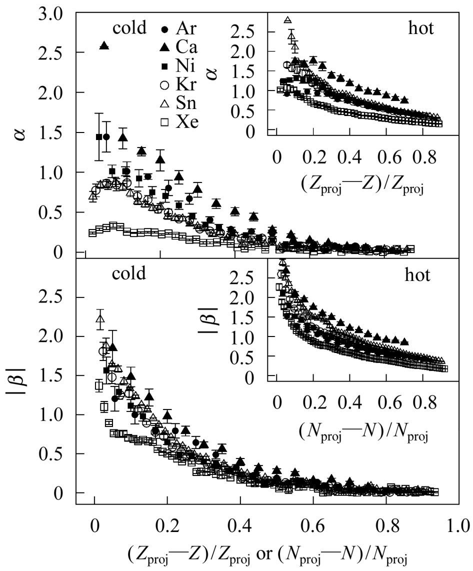

Fig. 4. The same as Fig. 2 but for the isoscaling parameters α as a function of $(Z_{\rm proj}-Z)/Z_{\rm proj}$ (upper panel) and $|\beta|$ as a function of $(N_{\rm proj}-N)/N_{\rm proj}$ (lower panel).

According to Eqs. (2) and (3), α and $|\beta|$ depend on $\Delta[(Z/A)^2]$ or $\Delta[(N/A)^2]$. Since this parameter is dependent on the reaction system, we divide $\alpha(|\beta|)$ by $\Delta[(Z/A)^2]$ $(\Delta[(N/A)^2])$ to remove the system isospin and size dependences and call them reduced isoscaling parameters. The results are given in Fig. 5. After the reduction, $\alpha/\Delta[(Z/A)^2]$ of different reaction systems demonstrates almost the same dependence with $(Z_{\rm proj}-Z)/Z_{\rm proj}$. $\beta/\Delta[(N/A)^2]$ also shows similar behavior. Eqs. (2) and (3) are deduced from the grand-canonical limit for multifragmentations of hot source. But for projectile-like fragments, the same behavior is observed in the SAA model. Thus $\alpha/\Delta[(Z/A)^2]$ $(\beta/\Delta[(N/A)^2])$ may be used as a sensitive observable for measuring the excitation extent of projectile-like fragments during the collisions. In the insets, the reduced parameters are different among different size reaction systems which mainly stem from the nonequilibrium effect of the pre-fragments before evaporation. As we can see, the reduced isoscaling parameters $\beta/\Delta[(N/A)^2]$ show some differences when $(N_{\rm proj}-N)/N_{\rm proj}$ is small. Because in our calculations projectiles with the same Z is used, collisions to produce isotopes with the same charge in the two reaction systems will have similar impact parameter or temperature. It satisfies the condition for isoscaling. But the collisions to produce isotones with the same neutron number in the two reaction systems will have some difference in impact parameter or temperature. So some difference for the reaction system dependence exhibits. It suggests that projectiles with the same Z are more suitable for investigation of the isoscaling behavior for isotopes than isotones.

Of course, we shall point out that the first abrasion stage is mostly a fast geometrical abrasion stage and no equilibrium can be expected for the pre-fragments. These fragments are only intermediate stage products and will decay due to their excitation. However, in order to investigate the evaporation effect, we can do similar analysis as the isoscaling analysis for cold fragments after evaporation which is principally more strict in physical condition, such as the requirement of equilibrium[21].

To investigate dependence of the reduced isoscaling parameters on $(Z_{\rm proj}-Z)/Z_{\rm proj}$ or $({\rm N}_{\rm proj}-N)/N_{\rm proj}$ more quantitatively, an exponential decay function is used to fit the extracted points from all reaction systems. The results and the fitted functions are shown as the solid lines in Fig. 5. From the figure we found a good exponential dependence of $\alpha/\Delta[(Z/A)^2]$ $(\beta/\Delta[(N/A)^2])$ on $(Z_{\rm proj}-Z)/Z_{\rm proj}\times((N_{\rm proj}-N)/N_{\rm proj})$.

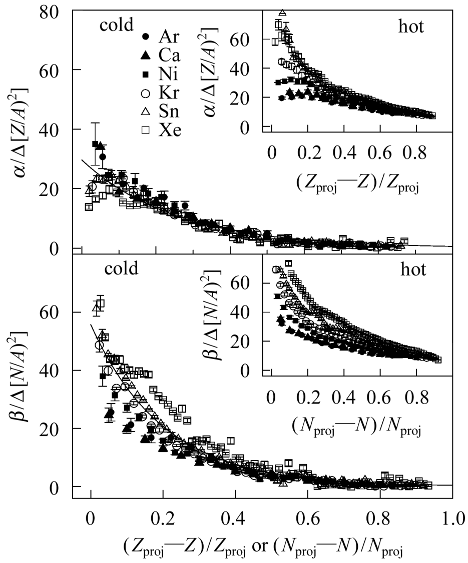

Fig. 5. The same as Fig. 4 but for the reduced isoscaling parameters $\alpha/\Delta[(Z/A)^2]$ (upper panel) and $\beta/\Delta[(N/A)^2]$ (lower panel). The solid lines are the fitted results by an exponential decay function.

From the above discussions, we find that $\Delta A_{\rm peak}/\Delta A_{\rm proj}$ and $\alpha/\Delta[(Z/A)^2]$ $(\beta/\Delta[(N/A)^2])$ decrease with $(Z_{\rm proj}-Z)/Z_{\rm proj}$ $((N_{\rm proj}-N)/N_{\rm proj})$ as an exponential function. But the latter one decreases slower than the first one. It means that $\alpha/\Delta[(Z/A)^2]$ $(\beta/\Delta[(N/A)^2])$ is more sensitive to the isospin effect of the projectiles. Since $\alpha/\Delta[(Z/A)^2]$ $(\beta/\Delta[(N/A)^2])$ is related to $\dfrac{C_{\rm sym}}{T}$, thus it can be used as an observable to study the excitation and asymmetric nuclear equation of state in heavy ion collisions.

4 Summary

In summary, systematic behaviors of the isospin effect and isoscaling of projectile-like fragments from $^{40/36}$Ar, $^{48/40}$Ca, $^{64/58}$Ni, $^{86/78}$Kr, $^{124/112}$Sn and $^{129/136}$Xe on ^{112}Sn at 60A MeV have been studied by a modified statistical abrasion-ablation model. The

peak positions of each isotopes and isotones are extracted. The normalized peak difference $\Delta A_{\rm peak}/\Delta A_{\rm proj}$ for different reaction systems shows similar dependence with $(Z_{\rm proj}-Z)/Z_{\rm proj}$. The isoscaling parameters α and β are extracted for the pre-fragments and final fragments and they show that different system has different value. But the reduced isoscaling parameters $\alpha/\Delta[(Z/A)^2]$ and $\beta/\Delta[(N/A)^2]$ for cold fragments show the same dependence with $(Z_{\rm proj}-Z)/Z_{\rm proj}$ or $(N_{\rm proj}-N)/N_{\rm proj}$ for different systems. The evaporation effect on the isospin effect and isoscaling parameters are discussed.

References

1 Bowman J D, Swiatecki W J, TANG C F. Lawrence Berkeley Laboratory Report No. LBL-**2908**, 1973

2 Hufner J, Shafer K, Schurmann B. Phys. Rev., 1975, **C12**: 1888

3 Gosset J et al. Phys. Rev., 1977, **C16**: 629

4 Morrissey M J et al. Phys. Rev., 1978, **C18**: 1267

5 Dayras R et al. Nucl. Phys., 1986, **A460**: 299

6 Bonasera A, Toro M D, Gregoire C. Nucl. Phys., 1987, **A463**: 653

7 Brohm T, Schmidt K H. Nucl. Phys., 1994, **A569**: 821

8 Tanihata I et al. Phys. Rev. Lett., 1985, **55**: 2676; Phys. Lett., 1985, **B160**: 380

9 Tanihata I et al. Phys. Lett., 1988, **B206**: 592

10 Miller M L et al. Phys. Rev. Lett., 1999, **82**: 1399

11 Dempsey J F et al. Phys. Rev., 1996, **C54**: 1710

12 LI B A et al. Phys. Rev. Lett., 1996, **76**: 4492

13 LI B A, Ko C M, Baur W. Int. J. Mod. Phys., 1998, **E7**: 147

14 Pak R et al. Phys. Rev. Lett., 1997, **78**: 1022; **78**: 1026

15 Kumar S et al. Phys. Rev., 1998, **C58**: 3494

16 Müller H, Serot B D. Phys. Rev., 1995, **C52**: 2072

17 MA Y G et al. Phys. Rev., 1999, **C60**: 024607

18 FANG D Q et al. Phys. Rev., 2000, **C61**: 044610; HEP & NP, 2000, **24**: 949 (in Chinese)
(方德清等. 高能物理与核物理, 2000, **24**: 949)

19 FANG D Q et al. Eur. Phys. J., 2001, **A10**: 0381

20 Tsang M B et al. Phys. Rev. Lett., 2001, **86**: 5023

21 Tsang M B et al. Phys. Rev., 2001, **C64**: 041603

22 Tsang M B et al. Phys. Rev., 2001, **C64**: 054615

23 Botvina A S, Vlozhkin O, Trautmann W. Phys. Rev., 2002, **C65**: 044610

24 Baran V et al. Phys. Rep., 2005, **410**: 335

25 MA Y G, SHEN W Q. Nucl. Sci. Tech., 2004, **15**: 4

26 MA Y G et al. Phys. Rev., 2004, **C69**: 064610

27 TIAN W D et al. Chin. Phys. Lett., 2005, **22**: 306

28 Fevre A L et al. Phys. Rev. Lett., 2005, **94**: 162701

29 Souliotis G A et al. Phys. Rev., 2006, **C73**: 024606

30 Souliotis G A et al. Phys. Rev., 2003, **C68**: 024605

31 Friedman W A. Phys. Rev., 2004, **C69**: 031601(R)

32 Veselsky M, Souliotis G A, Jandel M. Phys. Rev., 2004, **C69**: 044607

33 WANG K et al. Chin. Phys. Lett., 2005, **22**: 53

34 MA Y G et al. Phys. Rev., 2005,**C72**: 064603

35 Gaimard J J, Schmidt K H. Nucl. Phys., 1991, **A531**: 109

36 CAI X Z et al. Phys. Rev., 1998, **C58**: 572

37 ZHONG C et al. HEP & NP, 2003, **27**: 39 (in Chinese)
(钟晨等. 高能物理与核物理, 2003, **27**: 39)

38 Sfienti S et al. ACTA Physica Polonica, 2003, **B37**: 193

弹核碎裂反应中同位旋效应的系统研究*

方德清[1)] 马余刚 马春旺 钟晨 蔡翔舟 陈金根
郭威 苏前敏 田文栋 王鲲 颜廷志 沈文庆

(中国科学院上海应用物理研究所 上海 201800)

摘要 用统计擦碎模型对中能区不同弹靶体系在弹核碎裂反应中的同位旋效应和同位旋标度率现象进行了系统研究. 发现归一的同位素分布峰位差和约化的同位旋标度率参数随$(Z_{\rm proj}-Z)/Z_{\rm proj}$ or $(N_{\rm proj}-N)/N_{\rm proj}$ 呈指数下降, 与反应系统大小无关. 指出约化的同位旋标度率参数可以用来研究中能重离子碰撞中反应系统的激发程度和非对称核物质的状态方程.

关键词 统计擦碎模型 弹核碎裂反应 同位旋效应

2006 – 04 – 21 收稿, 2006 – 06 – 27 收修改稿

∗ 国家自然科学基金(10405032, 10535010, 10405033, 10475108, 10328259, 10135030), 上海市科技启明星(06QA14062, 05XD14021, 03QA14066)和国家重点基础研究发展规划项目(G200077404)资助

1) E-mail: dqfang@sinap.ac.cn